

## Natural History of Dot-like Cavernous Malformations (Telangiectasia) in Children with Medulloblastoma Treated with Radiation Therapy

Gordan Grahovac<sup>1</sup>, Tatiana Pundy<sup>1</sup>, Wadhvani Nitin<sup>2</sup> and Tadanori Tomita<sup>1</sup>

<sup>1</sup>Division of Neurosurgery, Ann and Robert H. Lurie Children's Hospital of Chicago, Northwestern University Feinberg School of Medicine, USA

<sup>2</sup>Department of Pathology, Ann & Robert H. Lurie Children's Hospital of Chicago, USA

Received February 17, 2016; Accepted April 11, 2016; Published July 6, 2016

### ABSTRACT

**Object:** This retrospective study was undertaken to define the prevalence of cavernous malformations (CM) or CM-like lesion in children with medulloblastoma who were postoperatively treated with radiation therapy (RT). We also aimed to clarify the natural history of radiation induced CM or CM-like lesions.

**Methods:** The authors reviewed medical records of 37 children with medulloblastoma, who underwent surgical resection, chemotherapy and RT during the period of 2002 to 2010. RT was applied with cumulative doses ranging from 5400-5860cGy to the primary posterior fossa with cranio-spinal axis doses <2340 cGy or >2340 cGy depending on tumor staging. The patients were consecutively followed with magnetic resonance (MR) imaging that included the 1.5 T or 3 T MRI modalities. The diagnosis of CM or CM like lesions was done based on four-tier Zabramski classification (Type I – IV).

**Results:** Thirty seven patients were followed up for 5.2 years on average (SD 2.5 years). Among 37 patients, who received RT, 8 patients (21.7%) did not develop any cavernous malformations. Mean age at the time of radiation therapy was 9.2 years (SD: 4.7 years). Twenty seven patients had type IV (dot-like CM) lesions and the remaining two patients developed the type I. There were no type II or III in this series. Only one of the type I developed symptoms (seizures) referable to the cavernous angioma which was surgically removed. Latency interval between radiation therapy and the development was 2.7 years on average (SD: 1.45 years). Even though type IV or dot-like CM location occurred in any location in the brain, majority of the lesions could be detected in the white gray junction in the cerebrum. Both type I lesions were detected in the cerebrum. Ten patients had the one to three lesions, 14 had four to six lesions, 3 had seven to nine lesions and 2 had more than 10 lesions. Histology of two dot-like CM of type IV at autopsy showed telangiectasia.

**Conclusion:** The development of dot-like CM is quite common after RT for medulloblastoma in childhood. GRE weighted images were superior to conventional T1-, T2- weighted images in detection of CMs and CM-like lesions. The SWI weighted images were statistically significantly superior to GRE weighted images in detecting dot-like CM affecting both supratentorial and infratentorial compartments. These dot-like lesions are mostly clinically silent telangiectasia, and rarely progress to hemorrhagic cavernous angioma.

**Keywords:** Cavernoma, Medulloblastoma, Radiation therapy

### INTRODUCTION

Radiation therapy (RT) is an integral part of the treatment of pediatric patients with malignant brain tumors. In recent years, use of this treatment modality contributed to longer patients' survival but also underscore the importance of awareness of long-term complications caused by RT and how they might affect patients' management during extended periods of observation.

Well-known early and late complications of RT such as brain atrophy, white matter necrosis, edema, demyelination, dystrophic mineralization and vascular abnormalities were described extensively in the past [1,2].

Vascular complications are late sequels of RT and they

include cerebrovascular accidents, lacunar lesions, vascular

**Corresponding author:** Tadanori Tomita, MD, Division of Neurosurgery, Ann and Robert H. Lurie Children's Hospital of Chicago, Chicago, IL 60611, USA, Tel: 312-227-442220; Fax: 312-227-9670; Email: ttomita@luriechildrens.org

**Citation:** Grahovac G, Pundy T, Nitin W & Tomita T (2016) Natural History of Dot-like Cavernous Malformations (Telangiectasia) in Children with Medulloblastoma Treated with Radiation Therapy J Neurosurg Imaging Techniques, 1(2): 66-75.

**Copyright:** ©2016 Grahovac G, Pundy T, Nitin W & Tomita T. This is an open-access article distributed under the terms of the Creative Commons Attribution License, which permits unrestricted use, distribution, and reproduction in any medium, provided the original author and source are credited.

occlusive disease including moyamoya syndrome, hemorrhage and vascular malformations. [3,4]. Vascular malformations are represented by telangiectasia, cavernous malformation (CM) and aneurysm. Little is known how telangiectasia and CM occur and how they are linked together.

There are several reports in the current literature related to the development of post-radiotherapy CM but only few publications of cerebral dot-like cavernous malformations can be found [5-9]. Rigamonti et al reported that capillary telangiectasia and cavernous malformations are a spectrum within a single pathological entity [10]. Zabramski classified the same telangiectatic changes previously reported by Rigamonti et al. into type IV changes in his four tier classification system of cerebral cavernous malformations [11].

The aim of this study is to describe the incidence of dot-like cavernous malformations in pediatric population of patients with medulloblastoma who underwent chemo and radiation therapy.

## MATERIAL AND METHODS

We retrospectively reviewed a cohort of 45 children with medulloblastoma, postoperatively treated with RT and chemotherapy at a single institution in order to elucidate the pathophysiology of the natural history of dot-like cavernous malformations and cavernous malformations. This group of patients underwent frequent magnetic resonance (MR) imaging follow up for the detection of recurrent tumor and gradient echo sequence (GRE) or susceptibility weighted imaging (SWI) were part of the established follow up imaging protocol intended to identify possible radiation induced late effect such as radiation-induced CM.

The brain tumor database at the Ann & Robert H. Lurie Children's Hospital of Chicago was reviewed to retrieve the data between 1 January, 2002 and 31, December 2010 and to identify all the patients with medulloblastomas, who underwent surgical resection, followed by radiation and chemotherapy and who have undergone the long-term imaging surveillance at this single institution.

Institutional Review Board approval (IRB#2005-12692) was obtained prior the retrieval of clinical and radiographic data. All patients were diagnosed before 18 years of age, and had long-term MR imaging surveillance. A retrospective charts review was performed and patients' clinical and demographic data were collected. All patients were followed clinically and radiologically at different intervals, beginning at 3 months postoperatively with follow up radiological examination repeated every 3 for the first 2 year, then every 4 to 6 months till the 5<sup>th</sup> year, then yearly depending on status of the disease.

Preoperatively every patient obtained the MR imaging studies of the head on 1.5 T or 3.0 T magnet. The imaging

included T1-, T2-, GRE, SWI and triplanar post gadolinium contrasted T1 weighted.

Neuro-imaging studies were reviewed for the presence, number, size, and anatomic location of dot-like cavernous malformation and CM. Follow up MR imaging studies were also obtained on a 1.5 T and/or 3.0 T magnet, and included axial T1-, T2-, and GRE, SWI and triplanar post gadolinium contrasted T1 weighted images.

The diagnosis of CM was done based on four-tier Zabramski classification; Type I-III are visible on at T1-, T2-weighted imaging [11], whereas Type IV, the dot-like cavernoma-like lesion, is visualized only on GRE or SWI weighted images (**Table 1**). Pathology review of the specimens from two autopsies was completed for evaluation of dot-like cavernoma.

Statistical analysis was done with the use of SPSS 11 software, and statistical significance was defined as p value < 0.05.

## RESULTS

Between 2002 and 2010, a total of 45 patients (28 male and 17 female) with medulloblastoma had surgical resection for their primary tumors at our institution. Out of 45 patients, 37 received both RT and chemotherapy, and were included in the study cohort for further analysis. None had familiar history of cavernomatosis. Of these 37 patients, 5 received proton beam therapy with cumulative dose of 54GyRBE and the remaining 32 received standard external beam RT with cumulative doses ranging from 5400-5860cGy to the primary posterior fossa site. To the cranio-spinal axis with doses ranging from 23.6 GyRBE to 36 GyRBE by Proton or 2340 cGy to 3600 cGy by external beam RT depending on tumor staging.

At the initial tumor presentation, preoperative MR of the brain did not reveal CM in any patients. The surveillance neuro-imaging in this study included the 1.5 T or 3 T MRI. Thirty seven patients were followed up radiologically and clinically for 5.2 years on average (SD 2.5 years).

Among 37 patients, who received RT, 8 patients (21.7%) did not develop any CMs. However, the mean follow up period was short, 2.8 years SD 2.7 years) among this cohort. Among this group -7 patients received standard external beam RT and 1 patient received proton beam therapy. Furthermore, 4 patients in this cohort did not have sufficient length of observation period because of the disease progression and early death within couple of months following completion of RT. Another patient transferred to another institution for the follow up care after RT and, subsequently, was lost to follow up. Mean age at the time of RT was 9.2 years with standard deviation (SD) of 4.7 years. The latency interval between the completion of RT and the development of CMs or CM-like lesion was 2.7 years (SD:

1.5years). MR imaging revealed Zabramski type IV lesions (dot-like cavernoma) in all except for 2 (**Figure 1**).

**Table 1.** Magnetic resonance imaging (MRI) signal characteristic of cerebral cavernomatous malformations (Zabramski et al, 1994)

Lesion type	MRI signal characteristics	Pathological characteristics
<b>Type I</b>	T1: hyperintense core T2: hyper- or hypointense core with surrounding hypointense rim	subacute hemorrhage, surrounded by a rim of hemosiderin-stained macrophages & gliotic brain
<b>Type II</b>	T1: reticulated mixed signal core T2: reticulated mixed signal core with surrounding hypointense rim	Loculated areas of hemorrhage & thrombosis of varying age, surrounded by gliotic, hemosiderin-stained brain; in large lesions, areas of calcification may be seen
<b>Type III</b>	T1: iso- or hypointense core T2: hypointense with a hypointense rim that magnifies the size of the lesion GE: hypointense with greater magnification than T2	chronic resolved hemorrhage, with hemosiderin staining within & around the lesion
<b>Type IV</b>	T1: poorly seen or not visualized at all T2: poorly seen or not visualized at all GE: punctate hypointense lesions	lesions that have been pathologically documented to be telangiectasias

Among those 29 patients with type IV or dot-like lesions, 5 patients had CM lesions in both supratentorial and infratentorial areas. Even though dot-like lesions occurred anywhere in multiple locations of the brain, majority of the lesions were detected in the white-gray junction or white matters in the cerebrum. The numbers of the CM lesions were as follows: 10 patients had one to three lesions, 14 had four to six lesions, 3 had 7 lesions and 2 had greater than 10 lesions (**Figure 2**). The number of the lesions may increase the first 6 to 18 months after detection but subsequently they become stabilized.

Two patients had type I lesion. Only one of them developed symptom: he had sudden onset of seizure due to a lesion in left temporal parietal region and because of persistent nature of seizures he was subjected to surgical resection (**Figure 3**). This patient had only solitary cavernous angioma.

Both GRE and SWI weighted images were superior to conventional T1-, T2- weighted images in detection of cavernous malformations. SWI is a 3D high-spatial resolution fully velocity corrected GRE. Both are sensitive to detect compounds of paramagnetic, diamagnetic and ferromagnetic properties. However, the SWI weighted images were statistically significantly superior to GRE weighted images in detecting dot-like cavernous malformation in supratentorial and infratentorial compartments. We had 26 instances where both GRE and SWI sequences were recorded. These were compared using Mann-Whitney non-parametric test and significant differences were found in numbers of cavernomas in both infratentorial and supratentorial areas ( $p \leq .0001$ ) (**Table 2**).

Two patients who developed multiple dot-like cavernous malformations died during follow up due to

medulloblastoma progression. The brain of those two patients harvested at post-mortem examination was subjected to pathological examination. Pathology findings revealed dilated thin-walled vessels with scant intervening

brain parenchyma showing reactive gliosis and hemosiderin-laden macrophages. An EVG stain shows no evidence of internal elastic lamina in the vessels. These findings are compatible with telangiectasia (Figure 4a, 4b).

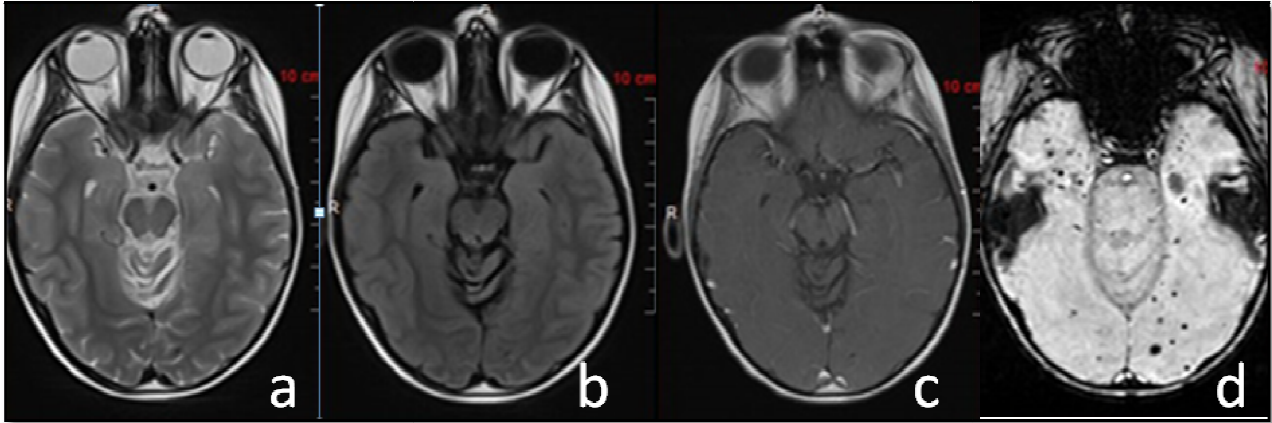


**Figure 1.** Axial MR images of multiple type 4 or dot-like cavernomas. T2-weighted (a), FLAIR (b), T1-weighted with contrast (c) and SWI (d). Note no or little visualization of the lesions other than SWI image.

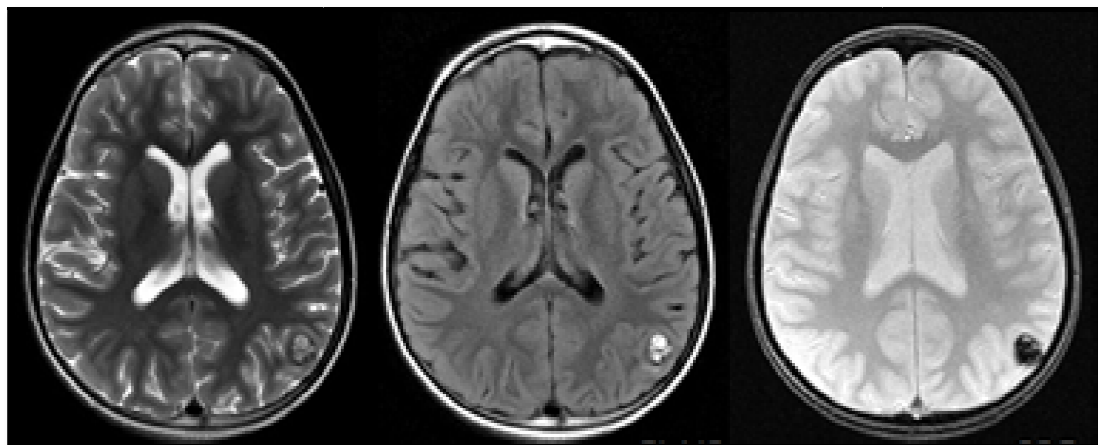


**Figure 2.** Axial MR images of Type 1 cavernoma. T2 weighted (Left), FLAIR (Center) and GRE (Right).

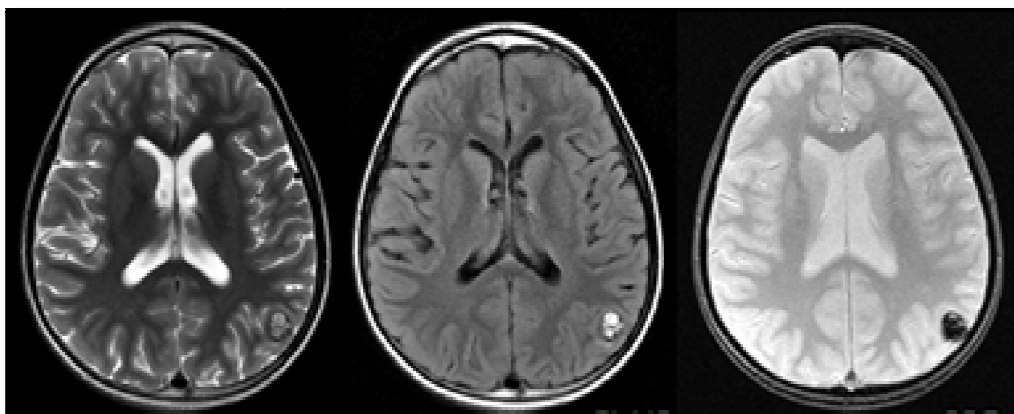


**Figure 3.** Multiple post-radiation cavernomas. GRE (left) and SWI (Right). Note SWI shows more sensitive to detect these lesions.

**Table 2.** GRE- SWI differences in numbers of detected cavernomas,  $p < .0001$ .

Brain area	Variable	N	Median	Lower Quartile	Upper Quartile	p value
Supratentorial	GRE cerebrum	26	4	3	6	$p \leq .0001$
	SWI cerebrum	26	8	5	17	
Infratentorial	GRE cerebellum	26	0.5	0	2	$p \leq .0001$
	SWI cerebellum	26	2	0	6	

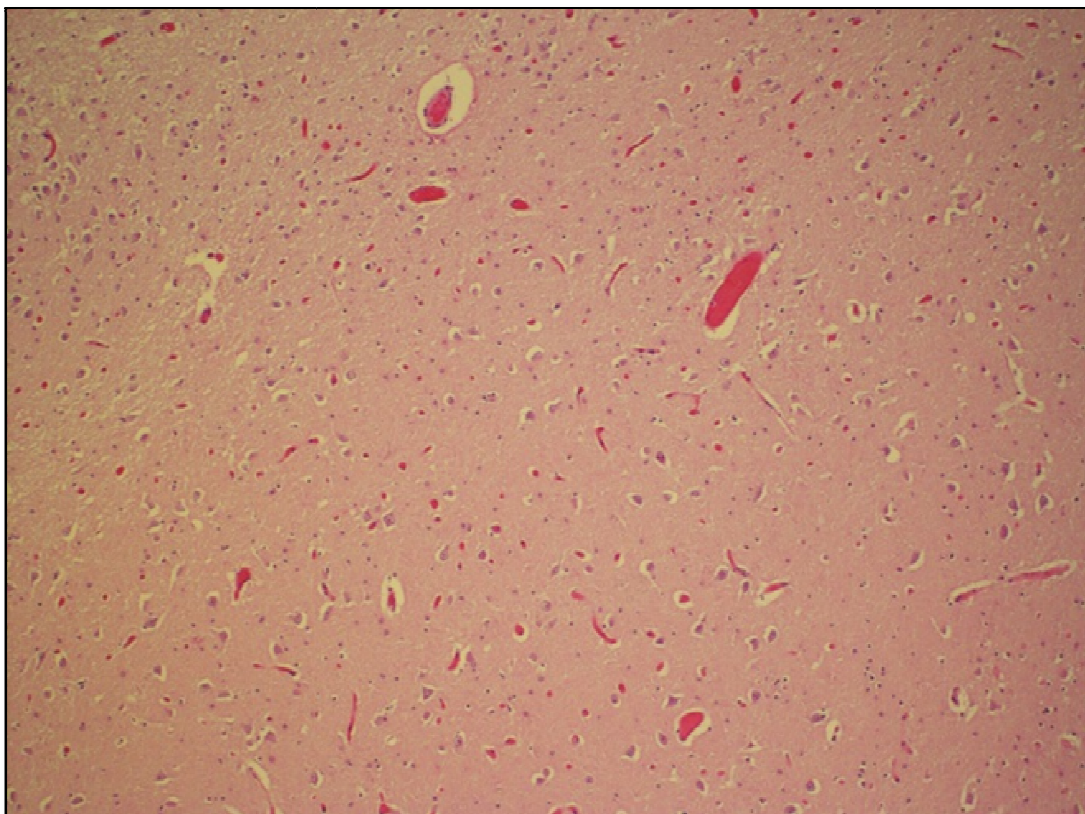


**Figure 4a.** Sections from the thalamic site show numerous small congested vascular spaces without an architectural organization (10x H&E).

Seven patients died of the progression of medulloblastoma; 3 early death as mentioned above and additional 4 patients 2.5, 4, 4 and 9 years after RT. One patient was lost to follow

up. All other 29 patients are alive from 5 to 13 years at the time of writing.

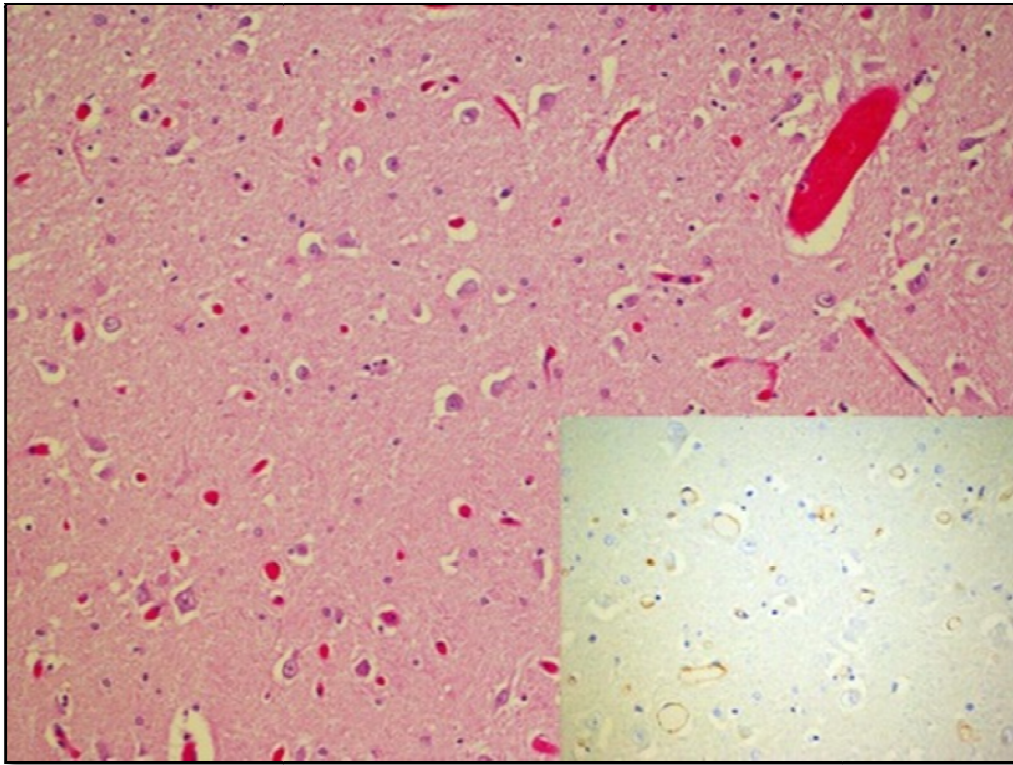


**Figure 4b.** At 20x magnification, an endothelial lining is more apparent. The CD31 immunostain (inset) shows reactivity for endothelial cells, confirming these are true endothelial lined capillaries.

## DISCUSSION

Cerebral CMs comprise 5%-13 % of all central nervous system vascular malformations with estimated prevalence in general population of 0.3-0.5% [12,13]. CM are blood cavities that are characterized by closely packed, thin wall enlarged vessels, lined by a single layer of endothelial cells without the muscular tissue or intervening brain parenchyma. CM are occult vascular lesions of the brain, and they are most commonly asymptomatic, but they might present with sudden onset of headache, seizure, hemorrhage or focal neurological deficit due to mass effect. The estimated risk for cerebral CM hemorrhage is 3.1 % per year and for seizure is 2.4% per year [14].

Cerebral CMs occur most commonly as sporadic lesions, and then patients usually have only one malformation. CM also might occur in familiar form, when few family members are affected, and then patient's presents with multiple cavernous malformations. Familial cases follow an autosomal dominant mode of inheritance and are caused by mutations in CCM1 (KRIT1), CCM2 (MGC4607), or CCM3 (PDCD10) genes. Somatic mutations within the three CCM

genes have been identified in CM lesions from both sporadic and familial patients. As 5 to 15% of familial CM cases remain still genetically unexplained [15].

Cranial radiation is main integral part of treatment for brain tumors, solid tumors of the head, and disorders with the involvement of central nervous system (CNS) such as brain metastases, and in cases when prevention of relapse of acute leukemia is warranted. Complications of the brain RT are well known and are related to the dose, fraction, and volume of irradiated brain, patient age, and concomitant therapy. According to the time of appearance we can divide the CNS reaction to the radiation to: 1) acute reactions that occurs during current radiation; 2) early delayed reactions, which appear from few weeks to 2 to 3 months after end of radiation therapy; and 3) late delayed reactions that can be manifested months to years after completion of the therapy [16].

Arteries and capillaries are especially sensitive to the radiation injury with veins being more resistant. It was shown in an animal model that approximately 15 % of

endothelial blood vessel cells were lost within 24 hours after radiation with dose of 5-200 Gy [17]. The direct consequence of radiation vasculature damage is a disruption of blood-brain barrier that causes vasogenic edema and tissue hypoxia. The endothelial loss is followed by thrombi formation and hemorrhage [18]. The vascular injury will lead to endothelial proliferation of injured vessels and formation of new vessels, basal membrane thickening, fibrosis of adventitia of blood vessels, and vessels dilation [19].

Many pro-inflammatory genes are upregulated within hours after radiation exposure such as tumor necrosis  $\alpha$ , interleukin- $1\beta$  and nuclear factor-kappa B [20]. Due to tissue hypoxia vascular endothelial growth factor (VEGF) is also elevated and has direct effect on development of new blood vessels [21].

Degree of the damage of the brain vessels is dose dependent and lower doses of radiation might not cause initial vessel damage. The effect of low radiation dose can be delayed 1-2 years after radiation exposure and can present with hemorrhagic infarct and telangiectasia formation [22,23].

Gaensler et al. published in 1994 their case series of 16 patients who underwent the whole brain irradiation as part of treatment protocol of primary brain tumors, with 14 patients being younger than 18 years old at the time of irradiation, who developed focal hypointense lesions on T2-weighted MRI images. Pathological examination of 6 patients with these lesions revealed small to larger regions of acute hemorrhage and revealed numerous thin-walled, ectatic vessels among normal neuropil elements. These lesions were considered to be telangiectatic changes [22].

Brain telangiectasias are dilated capillaries with thin endothelial walls, and are asymptomatic lesions of the brain with low vascular flow. Koike and al. followed 90 pediatric patients with the brain tumor who received RT with median follow up of 8.1 years with the MR. They found that 20 % of the patients developed telangiectatic changes and great majority was in the group who received more than 32 Gy of radiation. Half of the patients continued to develop additional new telangiectatic lesions 5 years after radiation [7].

First report of spontaneous hemorrhage, that developed in pediatric patients with brain tumors several years after craniospinal irradiation at the site away from brain tumor and revealed abnormal blood vessels in two of three patients, has been published in 1991 by Allen et al. [24]. Several years later Cirillo et al. [25] reported seven cases of cerebral CM in pediatric patients with brain tumor after craniospinal irradiation, with one patient that required surgical removal of hemorrhagic CM. Subsequently many other case studies and two-literature review of radiation-induced CMs, with review

of 85 and 72 cases respectively, have been published [26,27].

Zabramski et al. classified CMs into four-tier classification according to their histological and MR features [11]. Type I malformations are characterized by hyperintense core on T1 and hyper- or hypointensity core on T2-weighted sequences. In type II malformations, CMs exhibit a core with reticulated mixed signal intensity on T2-weighted sequences and on T1-weighted images, with a well-circumscribed hypointense rim on T2-weighted sequences. Type III malformations show a iso- or hypointensity on T1-weighted sequence and a hypointensity on T2-weighted sequence as well as a rim that is hypointense on T2-weighted sequences. Type IV malformations are punctate hypointense lesions on T2-weighted GRE MRI. Pathologic evaluation of the type I malformations revealed cavernoma that are consisted of subacute hemorrhages, type II malformations had hemorrhages and thrombosis of varying ages, and type III malformations had chronic hemorrhages with hemosiderin within and around the lesions. The pathology of type IV malformations can represent capillary telangiectasias or a CM in an early stage. Our two cases of brain autopsy of MR dot-like lesions on SWI sequence are confirming the theory of telangiectasias as type IV malformations.

Our data analysis shows that MR imaging is the best technique for evaluation of these occult vascular lesions. Cavernomas are best detected on T2 and GRE weighted images because of increased concentration of deoxyhemoglobin and hemosiderin. Increased concentration of deoxyhemoglobin is due to slow blood flow through cavernoma that leads to blood stagnation in the cavernas of the CM and increased extraction of the oxygen from the blood. Increased deposits of hemosiderin are due to microhemorrhages in and around CM. The hemosiderin deposits within and around the lesion together with susceptibility changes between deoxygenated blood and the surrounding brain tissue are causing signal loss that can be easily detected with GRE and SWI weighted sequence. Type III and type IV CM can be easily missed on conventional T1- and T2-weighted images [28, 29].

Detection of cavernomas also depends on the strength of the magnetic field, thickness of the section, and orientation of the section. Gold standard for detection of the cavernoma is still T2 and GRE weighted images. CM have typically "popcorn" or "mulberry" appearance with thin peripheral rim of decreased signal due hemosiderin deposit in the surrounding brain parenchyma [28,30].

The Zabramski classification published in 1994 [11] did not include the SWI in detection of CM lesions because SWI was introduced in 1997. Most recently many papers showed that SWI is more specific and sensitive for detecting dot-like cavernous malformations in familial cavernous

malformations. [30,31]. Our results also clearly showed that SWI is more sensitive for detecting RT induced dot-like cavernous lesions. Initially the lesions seen only on SWI were considered independently of the Zabramski classification system, but based on our research and pathology review findings that dot-like lesions correspond with the telangiectatic changes, we suggest that use of SWI technique warrants the update of Zabramski classification and recommend SWI as modality for detection of type IV lesion, since this method is more sensitive for small lesions that can be easily omitted with GRE sequence.

Measuring the diameter of the CM is possible only on T1- and T2 weighted imaging sequence, but the lesion diameter of the dot-like lesion is still clinical dilemma, since the appearance of the dot-like lesions is based on susceptibility artifact of the lesion that is proportionally dependent on the amount of hemosiderin deposit and technical aspect of the image acquisitions. So it is not advisable to measure the size of the lesion on SWI weighted imaging sequence.

Most recent study by de Champfleuret al. showed that dot-like cavernomas are best appreciated on the SWI weighted images; their numbers are significantly higher with SWI then with the T2 weighted images [32].

SWI is a technique that maximizes the sensitivity to susceptibility effects by combining a long-TE high-resolution fully flow-compensated 3D GRE sequence with filtered phase information in each voxel [29]. SWI has an exquisite sensitivity to the venous vasculature, blood products, and vascular malformations. Studies have suggested that SWI is more sensitive than T2-weighted imaging for evaluating CM [30,31]. In de Souza et al. series of familial CM SWI showed 73% more lesions than T2-weighted GRE images [30], and that was confirmed also by work of Bulut et al. [31]. In our series we have showed that the SWI was superior for detecting post radiation CM in both supratentorial and infratentorial parts of the brain tissue.

Yamasaki et al. [34] reported recently that of 25 patients with embryonal tumors (17 medulloblastomas, 5 primitive neuroectodermal tumors (PNET), 3 pineoblastomas) treated with craniospinal irradiation, 18 were alive and free of the recurrence. 14 patients developed CM in the course of a median of 56.7 months; 13 of these presented with multiple CMs. Patients who underwent RT at an age younger than 6 years developed multiple CMs significantly earlier than those treated at a later age ( $p=0.0110$ ). They found 4 patients with PNET/ pineoblastoma developed type 1 or 2 CM and significantly earlier than did 2 medulloblastoma patients ( $p=0.0042$ ) [34]. Our analysis of 37 medulloblastoma cases treated with RT revealed that earlier age at time of radiation therapy leads to more significant post-radiation damage of the brain Average age at time of

radiation leading to the development of type I lesions is 7.2 years old (SD: 4.4 years) versus 9.2 years old (SD: 4.0 years) leading to the development of Type IV lesions.

## CONCLUSIONS

Although post RT dot-like CMs or telangiectasia rarely cause symptoms like ours and others [6], they are common after RT for pediatric brain. Younger the patients when they receive RT, the higher the tendency of developing CMs. Advances in RT such as reduction of the radiation volume, new radiation protocols, use of proton beam therapy along with advent of new therapeutics such as bevacizumab (anti-VEGF agent) might cause less radiation related changes. Future studies might give us an answer if the new therapies might have less detrimental long-term effect on brain blood vessels, but this still needs to be elucidated.

## DISCLOSURE

The authors report no conflict of interest concerning the materials or methods used in this study or the findings specified in this paper.

## ACKNOWLEDGEMENT

We are grateful to Karen Rycklik, MS, from Biostatistics Research Core, Stanley Manne Children's Research Institute, for her help and guidance with statistical analysis of data.

## REFERENCES

1. Schultheiss TE, Stephens LC (1992) Invited review: permanent radiation myelopathy. *Br J Radiol* 65: 737-753.
2. Tomita T (1992) Long-term effects of treatment for childhood brain tumors. *Neurosurg Clin N Am* 3: 959-971.
3. Grenier Y, Tomita T, Byrd SE, Burrows DM, Marimond M (1998) Late Post-Radiation Occlusive Vasculopathy in Childhood Medulloblastoma: Report of 2 Cases. *J Neurosurgery* 89: 460-464.
4. Murphy ES, Xie H, Merchant TE, Yu JS, Chao ST, et al. (2015) Review of cranial radiotherapy-induced vasculopathy. *J Neurooncol* 122: 421-429.
5. Burn S, Gunny R, Phipps K, Gaze M, Hayward R (2007) Incidence of cavernoma development in children after radiotherapy for brain tumors. *J Neurosurg* 106: 379-383.
6. Di Giannatale A, Morana G, Rossi A, Cama A, Bertoluzzo L, et al. (2014) Natural history of cavernous malformations in children with brain tumors treated with radiotherapy and chemotherapy. *J Neurooncol* 117: 311-320.



7. Koike T, Yanagimachi N, Ishiguro H, Yabe H, Yabe M, Morimoto T, et al. (2012) High incidence of radiation-induced cavernous hemangioma in long-term survivors who underwent hematopoietic stem cell transplantation with radiation therapy during childhood or adolescence. *Biol Blood Marrow Transplant* 18: 1090-1098.
8. Lew SM, Morgan JN, Psaty E, Lefton DR, Allen JC, et al. (2006) Cumulative incidence of radiation-induced cavernomas in long-term survivors of medulloblastoma. *J Neurosurg* 104: 103-107.
9. Nikoubashman O, Wiesmann M, Tournier-Lasserre E, Mankad K, Bourgeois M, et al. (2013) Natural history of cerebral dot-like cavernomas. *Clin Radiol* 68: e453-459.
10. Rigamonti D, Johnson PC, Spetzler RF, Hadley MN, Drayer BP (1991) Cavernous malformations and capillary telangiectasia: a spectrum within a single pathological entity. *Neurosurgery* 28: 60-64.
11. Zabramski JM, Wascher TM, Spetzler RF, Johnson B, Golfinos J, et al. (1994) The natural history of familial cavernous malformations: results of an ongoing study. *J Neurosurg* 80: 422-432.
12. Kim DS, Park YG, Choi JU, Chung SS, Lee KC (1997) An analysis of the natural history of cavernous malformations. *Surg Neurol* 48: 9-17.
13. Labauge P, Brunereau L, Levy C, Laberge S, Houtteville JP (2000) The natural history of familial cerebral cavernomas: a retrospective MRI study of 40 patients. *Neuroradiology* 42: 327-332.
14. Kwon CS, Sheth SA, Walcott BP, Neal J, Eskandar EN, et al. (2013) Long-term seizure outcomes following resection of supratentorial cavernous malformations. *Clin Neurol Neurosurg* 115: 2377-2381.
15. Choquet H, Pawlikowska L, Lawton MT, Kim H (2015) Genetics of cerebral cavernous malformations: current status and future prospects. *J Neurosurg Sci* 59: 211-220.
16. Hylton PD, Reichman OH, Palutis R (1987) Monitoring of transient central nervous system postirradiation effects by <sup>133</sup>Xe inhalation regional cerebral blood flow measurements. *Neurosurgery* 21: 843-848.
17. Ljubimova NV, Levitman MK, Plotnikova ED, Eidus L (1991) Endothelial cell population dynamics in rat brain after local irradiation. *Br J Radiol* 64: 934-940.
18. Kortmann RD, Timmermann B, Taylor RE, Scarzello G, Plasswilm L, et al. (2003) Current and future strategies in radiotherapy of childhood low-grade glioma of the brain. Part I: Treatment modalities of radiation therapy. *Strahlenther Onkol* 179: 509-520.
19. Reinhold HS, Calvo W, Hopewell JW, van der Berg AP (1990) Development of blood vessel-related radiation damage in the fimbria of the central nervous system. *Int J Radiat Oncol Biol Phys* 18: 37-42.
20. Hong JH, Chiang CS, Campbell IL, Sun JR, Withers HR, et al. (1995) Induction of acute phase gene expression by brain irradiation. *Int J Radiat Oncol Biol Phys* 33: 619-626.
21. Li YQ, Ballinger JR, Nordal RA, Su ZF, Wong CS (2001) Hypoxia in radiation-induced blood-spinal cord barrier breakdown. *Cancer Res* 61: 3348-3354.
22. Gaensler EH, Dillon WP, Edwards MS, Larson DA, Rosenau W, et al. (1994) Radiation-induced telangiectasia in the brain simulates cryptic vascular malformations at MR imaging. *Radiology* 193: 629-636.
23. van der Kogel AJ (1986) Radiation-induced damage in the central nervous system: an interpretation of target cell responses. *Br J Cancer* 7: 207-217.
24. Allen JC, Miller DC, Budzilovich GN, Epstein FJ (1991) Brain and spinal cord hemorrhage in long-term survivors of malignant pediatric brain tumors: a possible late effect of therapy. *Neurology* 41: 148-150.
25. Ciricillo SF, Cogen PH, Edwards MS (1994) Pediatric cryptic vascular malformations: presentation, diagnosis and treatment. *Pediatr Neurosurg* 20: 137-147.
26. Keezer MR, Del Maestro R (2009) Radiation-induced cavernous hemangiomas: case report and literature review. *Can J Neurol Sci* 36: 303-310.
27. Nimjee SM, Keys JR, Pitoc GA, Quick G, Rusconi CP, et al. (2006) A novel antidote-controlled anticoagulant reduces thrombin generation and inflammation and improves cardiac function in cardiopulmonary bypass surgery. *Mol Ther* 14: 408-415.
28. Lehnhardt FG, von Smekal U, Ruckriem B, Stenzel W, Neveling M, et al. (2005) Value of gradient-echo magnetic resonance imaging in the diagnosis of familial cerebral cavernous malformation. *Arch Neurol* 62: 653-658.
29. Tomlinson FH, Houser OW, Scheithauer BW, Sundt TM, Okazaki H, et al. (1994)

- Angiographically occult vascular malformations: a correlative study of features on magnetic resonance imaging and histological examination. *Neurosurgery* 34: 792-799.
30. de Souza JM, Domingues RC, Cruz LC, Domingues FS, Iasbeck T, et al. (2008) Susceptibility-weighted imaging for the evaluation of patients with familial cerebral cavernous malformations: a comparison with t2-weighted fast spin-echo and gradient-echo sequences. *AJNR Am J Neuroradiol* 29: 154-158.
  31. Bulut HT, Sarica MA, Baykan AH (2014) The value of susceptibility weighted magnetic resonance imaging in evaluation of patients with familial cerebral cavernous angioma. *Int J Clin Exp Med* 7: 5296-5302.
  32. de Champfleury NM, Langlois C, Ankenbrandt WJ, Le Bars E, Leroy MA, et al. (2011) Magnetic resonance imaging evaluation of cerebral cavernous malformations with susceptibility-weighted imaging. *Neurosurgery* 68: 641-647.
  33. Sehgal V, Delproposto Z, Haacke EM, Tong KA, Wycliffe N, et al. (2005) Clinical applications of neuroimaging with susceptibility-weighted imaging. *J Magn Reson Imaging* 22: 439-450.
  34. Yamasaki F, Takayasu T, Nosaka R, Kenjo M, Akiyama Y, et al. (2015) The postirradiation incidence of cavernous angioma is higher in patients with childhood pineoblastoma or primitive neuroectodermal tumors than medulloblastoma. *Childs Nerv Syst* 31: 901-907.